Title	Parametric spectro-temporal analyzer (PASTA) for real-time optical spectrum observation
Author(s)	Zhang, C; Xu, J; Chui, PC; Wong, KKY
Citation	Scientific Reports, 2013, v. 3, p. article no. 2064
Issued Date	2013
URL	http://hdl.handle.net/10722/189011
Rights	Creative Commons: Attribution 3.0 Hong Kong License

SCIENTIFIC REPORTS

OPEN

SUBJECT AREAS:
SPECTROSCOPY
TRANSFORMATION OPTICS
NONLINEAR OPTICS
FIBRE OPTICS AND OPTICAL COMMUNICATIONS

Received
8 March 2013

Accepted
7 June 2013

Published
24 June 2013

Correspondence and requests for materials should be addressed to K.K.Y.W. (kywong@eee.hku.hk)

Parametric spectro-temporal analyzer (PASTA) for real-time optical spectrum observation

Chi Zhang, Jianbing Xu, P. C. Chui & Kenneth K. Y. Wong

Photonic Systems Research Laboratory, Department of Electrical and Electronic Engineering, The University of Hong Kong, Pokfulam Road, Hong Kong.

Real-time optical spectrum analysis is an essential tool in observing ultrafast phenomena, such as the dynamic monitoring of spectrum evolution. However, conventional method such as optical spectrum analyzers disperse the spectrum in space and allocate it in time sequence by mechanical rotation of a grating, so are incapable of operating at high speed. A more recent method all-optically stretches the spectrum in time domain, but is limited by the allowable input condition. In view of these constraints, here we present a real-time spectrum analyzer called parametric spectro-temporal analyzer (PASTA), which is based on the time-lens focusing mechanism. It achieves a frame rate as high as 100 MHz and accommodates various input conditions. As a proof of concept and also for the first time, we verify its applications in observing the dynamic spectrum of a Fourier domain mode-locked laser, and the spectrum evolution of a laser cavity during its stabilizing process.

The real-time spectrum observation is one of the most challenging tasks in the field of measurement, especially since the development of high-speed swept-sources[1]. It is also essential for the measurement of some non-repetitive events, such as the state evolution of a laser cavity[2], and dynamic chemical or physical systems[3], which usually occur in the time scale of nanosecond or microsecond. The bottleneck arises from the fact that, most conventional optical spectrum analyzers (OSAs) can only capture a few frames per second[4]. For example, the Czerny-Turner monochromator achieves fine resolution and high sensitivity, but is relatively slow for real-time applications[5]. Replacing this mechanical-scanning monochromator by a charge-coupled device (CCD) sensor as in the spectrometer enables faster operation (usually less than 1 kHz, but up to 1 MHz is feasible), but significantly compromises its accuracy[6]. Therefore, these methods based on spatial spreading of the spectrum can hardly be applied for real-time optical spectrum observation.

Recently, another method called amplified dispersive Fourier transformation (ADFT) was widely accepted in many ultrafast applications[7,8]. This concept was first introduced by Azana et al. for real-time Fourier transformation[9], where group-velocity dispersion (GVD) directly stretched spectra in the time domain. After wavelength-to-time mapping, the spectrum can be captured by a single-pixel detector and a real-time oscilloscope. However, for practical spectrum observation, two constraints still exist. First, the input condition of the signal is confined to short pulses. In particular, it usually operates in a passive manner, by launching a known wideband source into the ADFT to distinguish the absorption spectra, such as gaseous compounds[10]. Second, although Raman amplifier is incorporated to compensate the loss along the dispersive fiber[8], the pulse stretching is essentially an energy diverging process that inevitably degrades the detection sensitivity.

Here we study the possibility of achieving the all-optical wavelength-to-time mapping by a time-lens system[11], to overcome the aforementioned constraints. According to the Fourier optics, a two-focal-length (2*f*) configuration in the space-lens system performs the Fourier transformation between space and spatial frequency. Similarly, the time-lens counterpart can also achieve the transformation between time and frequency (wavelength), based on the space-time duality[12]. The time-to-frequency regime has been applied in an ultrafast temporal oscilloscope, which resolved the original temporal pulse shape on the spectrometer[13]. On the contrary, the wavelength-to-time regime has been applied for the ultrafast spectrum observation[14], and our work here is essentially developed from this concept.

Several methods have been developed to perform the time-lens, which can be primarily classified into two categories: quadratic signal onto a phase modulator[15], or a parametric mixer with chirped pump[16,17]. Although it is straightforward to implement by an electro-optic phase modulator, it cannot achieve large chirped range over a

long time span, and is usually operated with higher modulation bandwidth (5 GHz or above)[14,18]. If the observation window is wider (~ns), the parametric mixer configuration with larger pupil size and better effective duty ratio is more appropriate. The parametric mixer can be easily performed by a fiber-based $\chi^{(3)}$ system; the newly-generated idler will be imparted with twice the chirped range of the swept pump[19].

Based on this parametric time-lens, we present a real-time spectrum analyzer based on time-lens focusing mechanism, called parametric spectro-temporal analyzer (PASTA), with 100-MHz frame rate and 0.03-nm spectral resolution over 5-nm wavelength range. For an arbitrary waveform within the time-lens effective range, the PASTA can capture its spectrum, and revert the energy diverging process into converging process, thereby the detection sensitivity would be greatly enhanced. In view of the goal of achieving spectrum analysis with fine accuracy, PASTA provides a promising path to study the real-time spectrum of some dynamic phenomena and non-repetitive events, with orders of magnitude enhancement in the frame rate over conventional OSAs.

Results

Let us consider a scenario of an optical field with dynamic arbitrary spectrum along the time axis as shown in Fig. 1a. Based on the conventional OSA measurement, only the long-time (~200 ms) accumulated spectrum is obtained, and the detailed evolution of all the spectral components will be intertwined. When this optical field is launched into a PASTA that samples the spectrum in 10-ns intervals, these spectral components can be retrieved and lined up sequentially (Fig. 1a). Much like the fast movie frames, PASTA continuously captures and displays the spectral evolution. Here, the wavelength-to-time transformation of the PASTA system is essentially a time-lens focusing mechanism, based on the space-time duality[12] as shown in Fig. 1b and c. The time-lens introduces a quadratic phase shift or a linear frequency shift to the input signal in the time domain. Different wavelengths will be separated after the output dispersion, similar to the ADFT method[7]. When the output dispersion is equal to the focal dispersion of the time-lens, the linear frequency shift across the time-lens range can be compressed into a single temporal point[15,16]. Therefore, every single wavelength (parallel light beam with certain angle as shown in Fig. 1c) can be located on the one and only one position on the output time axis. In order to separate two closer spectral points (shown as the small angle or wavelength difference in Fig. 1c), larger focal dispersion of the time-lens and output dispersions are required. (For a quantitative description of the resolution and dispersion relation, see the Methods.)

There are two stages of four-wave mixing (FWM) involved in the time-lens implementation (Fig. 1d). The first-stage FWM is a parametric mixer with chirped pump, originated from a pump pulse with pulse width of 5 ps. The pump dispersion (−4 ns/nm) is provided by the dispersion-compensating fiber (DCF). If we directly focus the filtered idler after the first-stage FWM, the required output dispersion should be opposite to the pump dispersion, such as that provided by the single-mode fiber (SMF)[20]. However, it is noticed that DCF has much larger dispersion-to-loss ratio than standard SMF-28, which means SMF will provide the same amount of dispersion with larger insertion loss, and this is quite harmful in the case where large dispersion (2 ns/nm) is required. Therefore, another stage of FWM is inserted to perform as a phase conjugator (or spectral mirror)[21,22] with its spectral relation shown in Fig. 1e. The same DCFs can be utilized to chirp the pump and provide the output dispersion, so as to improve the detection sensitivity, and achieve better dispersion compensation or pulse compression[21].

A single continuous-wave (CW) source with a linewidth of less than 25 MHz was first tested by PASTA. In the ideal case, PASTA can compress the CW source into the initial pump pulse width (5 ps). However, considering the higher-order dispersion and limited acquisition bandwidth (16 GHz), the sharpest electrical pulse width that can be captured was 40 ps, which is shown as the eye diagram in Fig. 2a. The wavelength-to-time mapping relation was mainly determined by the output dispersion, which was −2 ns/nm (precisely −1.977 ns/nm), thus the single-shot wavelength resolution was calculated to be 0.02 nm. Besides, observing from Fig. 2a, the timing jitter was measured to be 20 ps, which degraded the resolution by another 0.01 nm. Therefore, the overall system resolution was 0.03 nm. The variation of peak power reflected the source stability, as well as the conversion efficiency of PASTA, since two

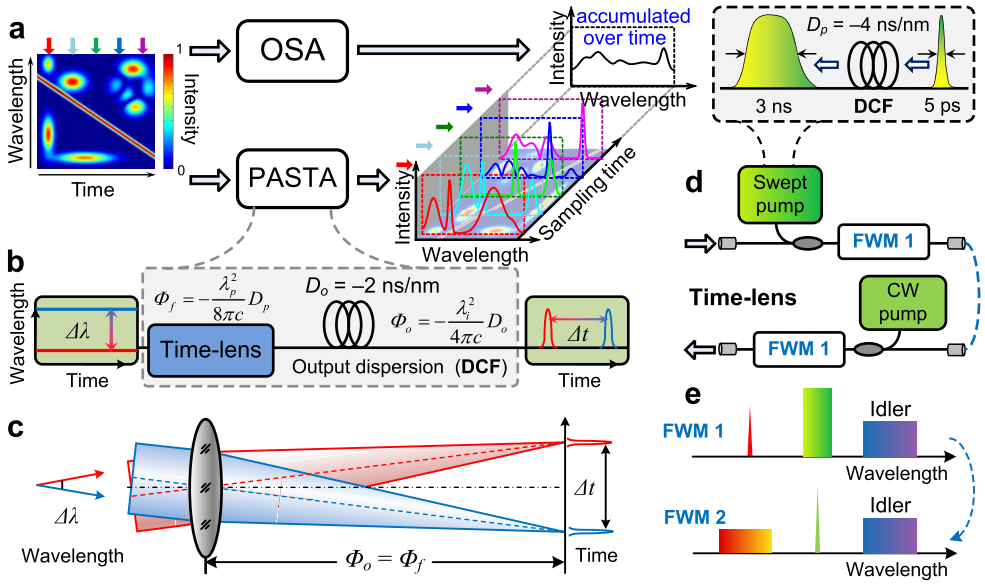

Figure 1 | Principle of the PASTA. An ultrafast spectrum analyzer is implemented using the time-lens focusing mechanism. (a) Conventional OSA vs. PASTA: OSA basically obtains the time-accumulated spectrum of that from PASTA. (b) PASTA performs the wavelength-to-time transformation by a time-lens and matched output dispersion. (c) Ray diagram[16] shows the time-lens focusing mechanism. (d) Time-lens is implemented by two stages of FWM. Short pulse passing through a dispersive fiber generates the swept-pump in the first-stage FWM, and the newly generated idler coupled together with a CW pump into the second-stage FWM. (e) The spectral relation along the two stages of FWM.

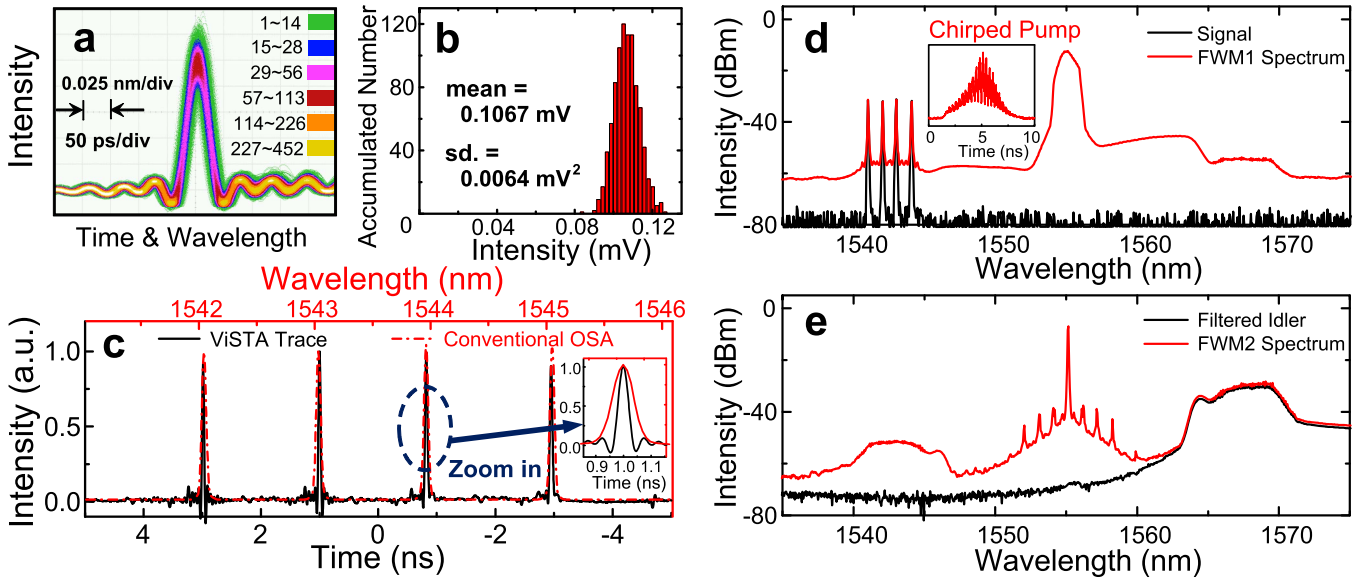

Figure 2 | Stationary characterization of PASTA. (a) Eye diagram of the PASTA spectrum obtained from a single CW laser. The color grade represents the number of sampling points accumulated within each pixel of the waveform viewing area. (b) Histogram of the peak power fluctuation of 900 consecutive pulses. (c) Four CW sources were approximately separated by 1 nm, and their spectra captured by a conventional OSA (red dash-dotted line) and the PASTA (black solid line). Inset: zoom-in spectrum of a single wavelength. (d & e) The spectra of the two stages of FWM, with (red) and without (black) the pump. Inset: temporal shape of the chirped pump.

stages of FWM were involved (Fig. 2b). The wavelength range of PASTA was determined by the repetition rate and the dispersion compensation bandwidth. The 100-MHz frame rate determined the 10-ns span for each period; divided by the wavelength-to-time relation (~2 ns/nm), the non-overlapping wavelength range could be 5 nm (from 1541 nm to 1546 nm). It was tested with four 1-nm spaced wavelengths, and the single-shot result is shown in Fig. 2c (black solid line), while the 10-ns time span corresponds to the 5-nm wavelength range. As a comparison, the same signal was measured by an OSA (Agilent 86142B) with a resolution of 0.06 nm (red dash-dotted line). These two measurements were in good agreement and the PASTA trace manifested better resolution (0.03 nm). The spectra of the two stages of FWM are shown in Fig. 2d and e, which also matched well with the spectral relation in Fig. 1e.

Comparing with the ADFT method, PASTA greatly relaxes the input conditions, from a short pulse (~ps or ~fs) to a long pulse (~ns) with arbitrary waveform. In the case of short input pulse, although it will not be focused by the time-lens, the linear frequency shift induced dispersion can compensate its time-shifting. In other words, time-shifting the position of the short pulse across the observation window will not affect the output spectrum. Therefore, pulse sources with different repetition rate can still be measured by PASTA without synchronization as in the case of ADFT. While for the longer input pulse (>1 ns), any waveform can be focused by the time-lens, and the inherent energy converging process contributes to its better detection sensitivity than ADFT as shown in Table 1. In general, the dynamic range of PASTA detection is limited by the amplified spontaneous emission (ASE) noise (lower power bound) and the gain saturation in the FWM conversions (upper power bound). These constraints limit the detection range from 1 μW (−30 dBm) to 1 mW, which correspond to a dynamic range of 1000 in our configuration. In addition to the detection sensitivity, since FWM is a polarization-sensitive process, the state-of-polarization (SOP) of the signal would also affect the conversion efficiency, which can be resolved by some polarization-diversity technique[23]. The performance comparison of PASTA versus other state-of-art spectrum-resolving technologies is summarized in Table 1, including conventional OSA[24], frequency-resolved optical gating (FROG)[25], Brillouin OSA (BOSA)[26], and the ADFT[7]. PASTA is definitely a promising candidate for ultrafast spectrum acquisition.

As a demonstration of the real-time spectrum observation capability of the PASTA, we used it to capture the dynamic spectrum of a fast swept-source, a Fourier domain mode-locked (FDML) laser, which had been widely employed in swept-source optical coherence tomography (SS-OCT) imaging modality[1]. The detection depth of SS-OCT is determined by the linewidth of the FDML source, which is

Table 1 | Performance of PASTA versus different technologies

Specifications	OSA[24] AQ6370C (Yokogawa)	FROG[25] FROG Scan (MesaPhotonics)	BOSA[26] (Aragon Photonics)	ADFT[7]	PASTA
Resolution	0.02 nm	0.2 nm	80 fm	~0.04 nm	0.03 nm
Wavelength range	100 nm	100–600 nm	37 nm	10 nm	5 nm
Sensitivity	−60 dBm [(1)]	>30 dBm	−70 dBm	>30 dBm	−30 dBm
Frame rate	5 Hz [(1)]	2 Hz	1 Hz	25 MHz	100 MHz
Input condition	Any	Short pulse (fs ~ ps)	Any	Short pulse (fs ~ ps)	Any
Observation time span	Any	30 ps	Any	~20 ms	~20 ms
Polarization	Any	Sensitive	Sensitive	Any	Sensitive [(2)]

[(1)]There is a trade-off between sensitivity and frame rate of the OSA, e. g. when sensitivity = −90 dBm, frame rate = 1/(75 sec) = 13.33 mHz.
[(2)]It can be solved by polarization-diversity technique[23].

usually measured by the roll-off method but is merely the averaged time-integrated linewidth. Another fast optical shutter based measurement can also analyze the linewidth at a certain point across the swept range, but it is still limited by the swept rate of OSA[27]. Here, the PASTA observed the real-time spectrum of such kind of FDML source, for the first time to the best of our knowledge. The FDML laser was constructed from a long fiber ring cavity (5-km SMF), a semiconductor optical amplifier (SOA), and a fiber Fabry-Perot tunable bandpass filter (FFP-TF). A 50-nm swept range centered at 1550 nm was demonstrated with 40-kHz effective swept rate. The wavelength band from 1541 nm to 1546 nm was filtered out, and evolution of the spectrum was obtained by the PASTA (Fig. 3a). Figure 3b shows the top view of the measured FDML spectra; the wavelength range of PASTA confined the observable swept bandwidth. Nevertheless, the observed sweeping within this range was essentially linear and the swept rate was 6.25 nm/μs, corresponding to the FFP-TF swept rate. To investigate the linewidth improvement by the mode-locking process, we compared the FDML laser with another swept ASE source, which was generated with a wide band ASE source passing through the FFP-TF under the same driving signal. The results are shown in Fig. 3c with similar sweeping feature except that the linewidth (from 0.08 nm to 0.25 nm) and the signal-to-noise ratio (SNR) were significantly degraded. It verified that the mode-locking process enables FDML to achieve narrower linewidth and better SNR.

To further demonstrate the PASTA's capability, we observed the spectrum evolution of a laser cavity during its stabilizing process. Here we set up a CW laser ring cavity, with a SOA as the gain medium, as illustrated in Fig. 4a. Generally speaking, this CW laser cavity takes less than 1 ms to reach the steady state[2]. To observe this non-repetitive process, it is required to actively control the starting point; therefore, an amplitude modulator (AM) was inserted as an optical shutter, or Q-switch of the cavity, with a passing time span of 1.25 ms. Since the cavity is around 10-m long, mode spacing is quite small, and multiple modes oscillating at the same time easily destabilize the output. The real-time intensity dynamics can be directly observed by a real-time oscilloscope, as shown in Fig. 4b; it took around 500 μs to reach the steady state. However, within such a short time span, it is hard to resolve the spectrum based on conventional

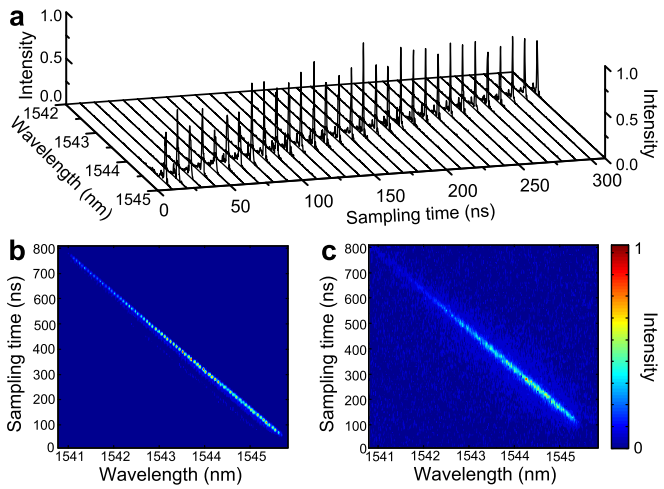

Figure 3 | Dynamic observation of the ultrafast swept-source. (a) Sequence of the FDML spectra movie frames acquired in a continuously sampling PASTA. (b) Top view of the same FDML dynamic spectra, and the color bar corresponds to the normalized spectral intensity (same as in (c)). The instantaneous linewidth is around 0.08 nm. (c) Top view of the spectral map of a swept ASE source. The instantaneous linewidth is around 0.25 nm, which agrees with the stationary bandwidth of the FFP-TF as specified.

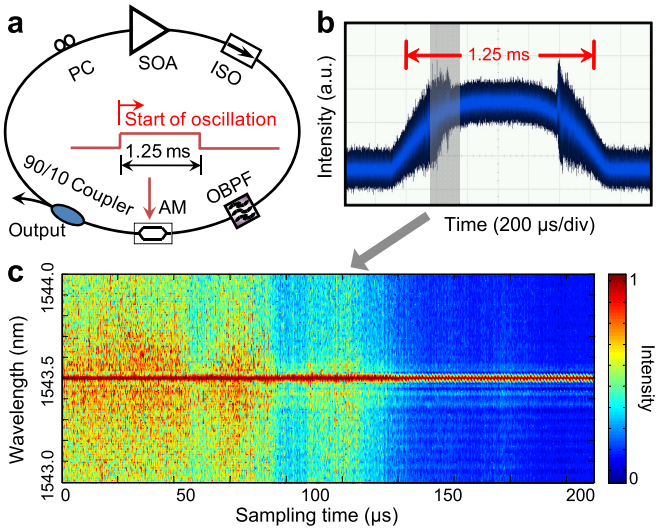

Figure 4 | Observation of the spectrum evolution of a laser cavity during its stabilization process. (a) Schematic setup of the laser cavity, with the filter bandwidth of 0.8 nm. Here, an AM acted as a Q-switch of the cavity was driven by a rectangular electrical signal, which controls the oscillation period. (b) Temporal intensity trace of the laser stabilization process. (c) Top view of the spectral map of the laser stabilization process within a 200-μs observation span (corresponds to the gray area in (b)).

instruments. Here, the PASTA, for the first time, observed the spectral evolution when the laser is reaching its steady state, as shown in Fig. 4c. To maintain the sampling rate of 80 GSa/s, the maximum observation span that can be captured by the real-time oscilloscope (Agilent DSO-X 91604A, 16-GHz bandwidth) is 256 μs, limited by its built-in 20.5-Mpts memory depth. Considering that Agilent provides the maximum memory depth of 2.1-Gpts[28], the observation span of PASTA can cover up to 26.25 ms.

Discussion

In conclusion, we report an ultrafast spectrum observation modality, PASTA, achieving the frame rate of 100 MHz based on the time-lens focusing mechanism. With focal dispersion of 2 ns/nm, this PASTA system has demonstrated a spectral resolution of 0.03 nm within a 5-nm wavelength range and even finer resolution can be achieved with a spectral magnification technique[29]. Arbitrary waveform (long pulse or short pulse) within the observation window can be measured, and the input condition is not as restrictive as other real-time measurement method such as ADFT. Owing to the inherent energy converging feature, it has achieved detection sensitivity as low as −30 dBm (1 μW), as well as over 1000 for dynamic range. In order to verify its ultrafast performance, we have used the PASTA to measure the dynamic spectrum of a FDML swept-source, and a laser cavity during its stabilization process. We were able to perform these real-time spectrum analyses for the first time, and we therefore expect that PASTA will find numerous applications in areas where rapid spectral acquisition is essential.

Methods

Set-up. The 5-ps pump pulse was generated by a 10-GHz mode-locked fiber laser with the central wavelength at 1555 nm, and its repetition rate was down-converted to 100 MHz by an external AM. A 16.3-km DCF spool was multiply used for the time-lens focusing: (1) for the 1555-nm pump branch, the 5-ps pump pulse passed this DCF twice to achieve the pump group-dispersion delay (GDD) of 2626 ps^2 (the chirped pump is shown as the inset of Fig. 2d); (2) for the 1543.5-nm output dispersion, the chirped signal passed this DCF once to achieve the output GDD of 1241 ps^2. Owing to the dispersion slope, the pump wavelength experienced a larger GDD. So we included another spool of 13.1-km SMF in the pump branch (−144 ps^2) to compensate the pump GDD to 2482 ps^2, and satisfy the time-lens focusing relation. The swept pump passed through a 3-nm bandwidth filter before the first-stage FWM,

while the second-stage FWM was pumped by a distributed feedback (DFB) laser. Two spools of highly-nonlinear dispersion-shifted fibers (HNL-DSFs), with the same zero-dispersion wavelength at 1554 nm, were employed as the nonlinear medium for FWM. Two erbium-doped fiber amplifiers (EDFAs) were inserted to compensate the low FWM conversion efficiency.

Dispersion and resolution. Neglecting the higher-order dispersion, the ideal output optical pulse width can be expressed as $\Delta t_o = 3.543\pi\Phi_f/T$, here Φ_f is the focal GDD, but it cannot be narrower than the transform-limited pump pulse width. On the other hand, any electrical device has limited detection bandwidth, and the shortest electrical pulse width should be $\Delta t_e = 2\ln 2/\pi f_{BW}$, where f_{BW} is the detection bandwidth. Here, the 16-GHz bandwidth corresponds to around 30-ps electrical pulse width, which is more critical in quantifying the spectral resolution. The following wavelength-to-time mapping relation can be used to calculate the spectral resolution: $\Delta\lambda = \Delta t \times \lambda^2/4\pi c\Phi_f$, where $\Delta t = \Delta t_e$ in our experiment.

Trigger signal. It is essential to calibrate multi-frames (separation and re-alignment), since all spectral frames are captured as an entire trace from the real-time oscilloscope. There are two approaches of obtaining this trigger signal: (a) directly obtained from the pump pulses, though it can only recover the relative spectral positions; (b) generated from a CW source with known wavelength into the PASTA, which can recover the precise spectral frames. Here, we employed the latter approach.

1. Huber, R., Wojtkowski, M. & Fujimoto, J. G. Fourier Domain Mode Locking (FDML): A new laser operating regime and applications for optical coherence tomography. *Opt. Express* **17**, 5691–5697 (2009).
2. Svelto, O. *Principles of Lasers* 4th edn (Plenum Press, 1998).
3. Petty, H. R. Spatiotemporal chemical dynamics in living cells: from information trafficking to cell physiology. *Biosystems* **83**, 217–224 (2004).
4. Derickson, D. *Fiber Optic, Test and Measurement* (Prentice Hall, 1998).
5. Shafer, A. B., Megill, L. R. & Droppleman, L. A. Optimization of the Czerny–Turner spectrometer. *J. Opt. Soc. Am.* **54**, 879–887 (1964).
6. Etoh, T. G. *et al.* Evolution of Ultra-High-Speed CCD Imagers. *Plasma and Fusion Res.* **2**, S1021 (2007).
7. Solli, D. R., Chou, J. & Jalali, B. Amplified wavelength-time transformation for real-time spectroscopy. *Nat. Photonics* **2**, 48–51 (2008).
8. Goda, K. & Jalali, B. Dispersive Fourier transformation for fast continuous single-shot measurements. *Nat. Photonics* **7**, 102–112 (2013).
9. Azana, J. & Muriel, M. A. Real-Time Optical Spectrum Analysis Based on the Time–Space Duality in Chirped Fiber Gratings. *IEEE J. Quantum Electron.* **36**, 517–526 (2000).
10. Chou, J., Han, Y. & Jalali, B. Time-wavelength spectroscopy for chemical sensing. *IEEE Photon. Technol. Lett.* **16**, 1140–1142 (2004).
11. Goodman, J. W. *Introduction to Fourier Optics* 3rd edn, (Roberts and Company Publishers, 2005).
12. Kolner, B. H. Space-Time Duality and the Theory of Temporal Imaging. *IEEE J. Quantum Electron.* **30**, 1951–1963 (1994).
13. Foster, M. A. *et al.* Silicon-chip-based ultrafast optical oscilloscope. *Nature* **456**, 81–85 (2008).
14. Berger, N. K., Levit, B., Atkins, S. & Fischer, B. Time-lens-based spectral analysis of optical pulses by electrooptic phase modulation. *Electron. Lett.* **36**, 1644–1646 (2000).
15. Kolner, B. H. Active pulse compression using an integrated electro-optic phase modulator. *App. Phys. Lett.* **52**, 1122–1124 (1988).
16. Bennett, C. V. & Kolner, B. H. Principles of Parametric Temporal Imaging—Part I: System Configurations. *IEEE J. Quantum Electron.* **36**, 430–437 (2000).
17. Bennett, C. V. & Kolner, B. H. Principles of Parametric Temporal Imaging—Part II: System Performance. *IEEE J. Quantum Electron.* **36**, 649–655 (2000).
18. van Howe, J., Lee, J. H. & Xu, C. Generation of 3.5 nJ femtosecond pulses from a continuous-wave laser without mode locking. *Opt. Lett.* **32**, 1408–1410 (2007).
19. Zhang, C., Cheung, K. K. Y., Chui, P. C., Tsia, K. K. & Wong, K. K. Y. Fiber Optical Parametric Amplifier with High-Speed Swept Pump. *IEEE Photon. Technol. Lett.* **23**, 1022–1024 (2011).
20. Agrawal, G. P. *Nonlinear Fiber Optics* 4th edn (Academic Press, 2007).
21. Gu, C., Ilan, B. & Sharping, J. E. Demonstration of nondegenerate spectrum reversal in optical-frequency regime. *Opt. Lett.* **38**, 591–593 (2013).
22. Yariv, A., Fekete, D. & Pepper, D. M. Compensation for channel dispersion by nonlinear optical phase conjugation. *Opt. Lett.* **4**, 52–54 (1979).
23. Wong, K. K. Y., Marhic, M. E., Uesaka, K. & Kazovsky, L. G. Polarization-Independent One-Pump Fiber Optical Parametric Amplifier. *IEEE Photon. Technol. Lett.* **14**, 1506–1508 (2002).
24. Yokogawa Optical Spectrum Analyzer, http://tmi.yokogawa.com/products/optical-measuring-instruments/optical-spectrum-analyzer/aq6370c-optical-spectrum-analyzer/ (Accessed 8th Mar 2013).
25. Real-Time Ultrafast Laser Pulse Measurement, http://www.mesaphotonics.com/products-2/pulse-measurement/frogscan/ (Accessed 8th Mar 2013).
26. BOSA High Resolution Optical Spectrum Analyzer, http://www.aragonphotonics.com/ficha.php?opt=2 (Accessed 8th Mar 2013).
27. Biedermann, B. R., Wieser, W., Eigenwillig, C. M., Klein, T. & Huber, R. Direct measurement of the instantaneous linewidth of rapidly wavelength-swept lasers. *Opt. Lett.* **35**, 3733–3735 (2010).
28. Agilent Real-Time Oscilloscope, http://cp.literature.agilent.com/litweb/pdf/5990-5271EN.pdf (Accessed 8th Mar 2013).
29. Okawachi, Y. *et al.* High-resolution spectroscopy using a frequency magnifier. *Opt. Express* **17**, 5691–5697 (2009).

Acknowledgements

The work was partially supported by grants from the Research Grants Council of the HKSAR, China (project HKU 717212E). The authors also acknowledge Sumitomo Electric Industries for providing the HNL-DSF. We are grateful to Prof. Michel Marhic and Dr. Nelson Chan for helpful discussions. We also thank Dr. Kevin Tsia for providing us with the real-time oscilloscope.

Author contributions

The experiment was designed and implemented by C. Zhang. The FDML source was developed by J. Xu. K. Wong and C. Zhang developed the concept. K. Wong and P. C. Chui supervised measurements and analysis. All authors contribute the preparation of the manuscript.

Additional information

Competing financial interests: The authors declare no competing financial interests.

How to cite this article: Zhang, C., Xu, J.B., Chui, P.C. & Wong, K.K.Y. Parametric spectro-temporal analyzer (PASTA) for real-time optical spectrum observation. *Sci. Rep.* **3**, 2064; DOI:10.1038/srep02064 (2013).